

Proceedings of the National Academy of Sciences

Annotated PDFs will now be accepted for proof return. Authors who would like to return their proofs by mail, please print all pages of the proof PDF (use “normal quality”). Note the following directions for correcting and returning your proofs. **Important:** For your convenience, this page contains a shortened version of the content in the proof notification e-mail, and some information is not repeated here. Please read the e-mail letter, which will inform you if your article exceeds our page limit.

Please note: The date a paper appears online in PNAS daily Early Edition is the publication date of record and is posted with the article text online. **All author changes must be made before the paper is published online or will be considered and processed as errata.**

Text

- 1) Clearly mark all of your changes and answers to author queries in the margins next to the article text in the proofs, either in the annotated PDF or on the hard copy;
- 2) Review and answer ALL author queries (marked in the margins of the text with AQ: A, etc.) that are listed on the query sheet(s);
- 3) Proofread tables and equations carefully; and
- 4) Make sure that any Greek/special characters appear correctly throughout the text.
- 5) PNAS charges for extensive author alterations on proofs. Six or more author alterations per page will be charged at \$4 each. Authors will not be charged to correct printer's errors, copyediting errors, or figure errors made in composition.

Figures

- 1) Proofs contain low-resolution figures (so proofs can be downloaded and printed quickly). Figure quality will be higher in the printed and online html versions of the journal. Please note any figure quality concerns next to the figure on the proofs.
- 2) Carefully check fig. numbering, color, text labeling, and cropping; if elements are missing from or moved within a figure, or if your color figure does not appear in color in the PDF, please note this on your proofs and send us a printed copy of the correct figure for comparison;
- 3) Replacing, deleting, or resizing color figures will cost \$150/figure and replacing a black-and-white figure will cost \$25/figure.

Supporting Information

PNAS charges for extensive author corrections in SI. Four or more author alterations per SI page will be charged at \$4 each. Replacing SI figs. will cost \$25/fig.

Within 2 business days, please either return your annotated proof PDF electronically to the editorial contact listed in query A of your proof, or express mail (by overnight or 2-day delivery, if possible) the following items to the address given below.

- 1) The original printed copy of the PDF, including query sheet(s), with your corrections marked in the margins next to the article text;
- 2) The reprint order form (including the price sheet). You can fax this form to the number listed on it instead of mailing the form back to us. If you have trouble printing the form, it is also available on our web site at http://www.pnas.org/misc/author_reprints.pdf.

Please retain a copy of ALL pages of the proof PDF for your records. Please include your manuscript number with all correspondence.

Thank you.

Return address for proofs:

Attn: PNAS

8621 Robert Fulton Dr., Suite 100

Columbia, MD 21046

pnas@cadmus.com

Tel: 410-850-0500 (Use this number for shipping purposes only; see query A on the Author Queries sheet in your proof PDF for contact information for your article.)

Golgi protein FAPP2 tubulates membranes

Xinwang Cao^a, Ünal Coskun^a, Manfred Rössle^b, Sabine Buschhorn^a, Michal Grzybek^a, Timothy Dafforn^c, Marc Lenoir^c, Michael Overduin^c, and Kai Simons^{a,1}

^aMax Planck Institute for Molecular Cell Biology and Genetics, Dresden, Germany; ^bEuropean Molecular Biology Laboratory EMBL, Hamburg Outstation c/o DESY, Hamburg, Germany; and ^cSchool of Cancer Sciences, University of Birmingham, Birmingham, United Kingdom

Contributed by Kai Simons, October 14, 2009 (sent for review October 7, 2009)

AQ: A The Golgi-associated four-phosphate adaptor protein 2 (FAPP2) has been shown to possess transfer activity for glucosylceramide both in vitro and in cells. We have previously shown that FAPP2 is involved in apical transport from the Golgi complex in epithelial

AQ: B MDCK cells. In this paper we assign a new activity for the protein as well as providing structural insight into protein assembly and a low-resolution envelope structure. By analyzing analytical ultracentrifugation and small-angle x-ray scattering (SAXS) data, FAPP2 is a dimeric protein in solution, with a molecular weight of 100 nm in length. The purified FAPP2 protein is able to form tubules from membrane sheets in a PI (4)P-dependent manner on the phosphoinositide-binding PH domain of FAPP2. These data suggest that FAPP2 is involved in the formation of apical carriers in the

membrane tubulation, PH domain, and trans-Golgi network

Fn1 Outgoing traffic from the Golgi complex diverges into different directions. In epithelial cells, one major route is to the apical membrane. The machinery responsible for the formation of apical carriers is poorly understood. Several proteins have been identified that play a role (1–3). One such protein is the Golgi-associated four-phosphate adaptor protein 2 (FAPP2) (4–6). FAPP2 is a cytosolic protein consisting of the following: an N-terminal pleckstrin homology (PH) domain recognizing the Golgi marker, phosphatidylinositol 4-phosphate [PI (4)P], followed by a central proline-rich region, and a glycolipid transfer protein (GLTP)-like domain toward the C terminus (4). Recent studies have shown that FAPP2 has transfer activity for glucosylceramide (GlcCer) both in vitro and in cells (7, 8). Knocking down FAPP2 by RNAi reduces the conversion of (GlcCer) to lactosylceramide (LacCer) and to downstream complex glycolipids and gangliosides. Evidence suggesting that FAPP2 regulates membrane transport from the Golgi by its glycolipid transfer function was also brought forward. However, the two papers give different directions for the transfer. D'Angelo et al. (7) favor a transfer of GlcCer from the *cis*-Golgi to the trans-Golgi, whereas Halter et al. (8) suggest that FAPP2 takes GlcCer from the trans-Golgi membrane to the endoplasmic reticulum. In the latter case, GlcCer would be flopped after its transfer to the luminal side to be transported to the Golgi complex, where it would function as a precursor for glycolipid biosynthesis. Thus, there is no consensus as to how FAPP2 would control exit of proteins from the trans Golgi network to the cell surface.

In this paper we explored other possible properties of FAPP2 and discovered that purified FAPP2 tubulates lipid membranes in a PI (4)P-dependent fashion. This finding would fit well with properties previously attributed to the protein (4) and adds an important missing function in the machinery responsible for apical transport. In addition, analytical ultracentrifugation (AUC) and small-angle x-ray scattering (SAXS) studies provide structural insights into the dimeric solution state and molecular shape of the full-length FAPP2 protein.

Results

Previous studies by Godi et al. have shown that expression of FAPP2 in Cos7 cells led to the formation of tubules from the

trans-Golgi network (4). To check whether this is also the case in MDCK cells, we expressed FAPP2 in these cells and could demonstrate that FAPP2 was indeed present in tubules forming from the trans-Golgi (Fig. S1C).

To explore this phenomenon further, we tested whether purified FAPP2 had tubulation activity in vitro. We first produced full-length canine FAPP2 having a glutathione S-transferase (GST) fusion at the N terminus in *E. coli*. The protein was purified to high-purity (Fig. S3B, control lanes) for analysis of its effects on membranes. In addition, an N-terminally tagged mCherry-FAPP2 protein was produced to monitor the location of FAPP2 on membranes.

Membrane Tubulation by FAPP2. The effect of FAPP2 on lipid membranes sheets was monitored in real time by light microscopy (9). A mix of POPC:PI (4)P:GlcCer (96:2:2 mol%) was spotted on a coverslip surface and dried. Injection of the soluble protein to the rehydrated membrane sheets induced growth of membrane tubules at the edges or on the top of the most superficial layer of the lipid sheets (Fig. 1A). Tubules coated with mCherry-FAPP2 grew away from the membrane lipid sheets, implying that the binding of FAPP2 to the membrane sheet induced positive curvature of the membrane (Fig. 1E).

Because FAPP2 binds PI (4)P via its PH domain and GlcCer through its GLTP domain, we investigated which lipids are required for membrane tubulation. Full-length FAPP2 tubulated membrane sheets in a PI (4)P-dependent manner, consistent with the capability of its PH domain to bind specifically to this phosphoinositide (10). Only PI (4)P and not GlcCer is required, as tubulation occurred with POPC and PI (4)P (98:2 mol %) (Fig. 1B), but not with either POPC alone (Fig. 1C) or with a mixture of POPC and GlcCer (98:2 mol%) (Fig. 1D).

As the ability of FAPP2 to tubulate membrane sheets appeared to be dependent on its PH domain and PI (4)P, we examined whether mutation of Arg-18 to a leucine residue (R18L) in the PH domain, which has been described to abolish Golgi localization of FAPP2 (4), would affect tubulation. Purified FAPP2-R18L mutant protein did not induce any detectable membrane tubulation (Fig. 2A and Movie S1), suggesting an inability to associate with, insert into, or bend membranes. When WT-FAPP2 was injected into the same chamber, tubules grew out from the membrane sheet immediately, indicating a “recovery” of activity at the membrane surface (Fig. 2B and Movie S2). Together this indicates that tubulation activity requires a functionally intact PH domain that can bind to PI (4)P.

The potential role of GlcCer in the tubulation activity was also assessed by mutating an essential Trp in the GLTP domain of FAPP2, disabling the protein to bind to GlcCer (7). The W407A mutant protein generated tubules from the membrane sheets,

Author contributions: X.C., Ü.C., M.L., M.O., and K.S. designed research; X.C., Ü.C., M.R., S.B., M.G., and T.D. performed research; M.L. and M.O. contributed new reagents/analytic tools; X.C., Ü.C., M.R., S.B., M.G., and T.D. analyzed data; and Ü.C. and K.S. wrote the paper.

The authors declare no conflict of interest.

¹To whom correspondence should be addressed. E-mail: simons@mpi-cbg.de.

This article contains supporting information online at www.pnas.org/cgi/content/full/0911789106/DCSupplemental.

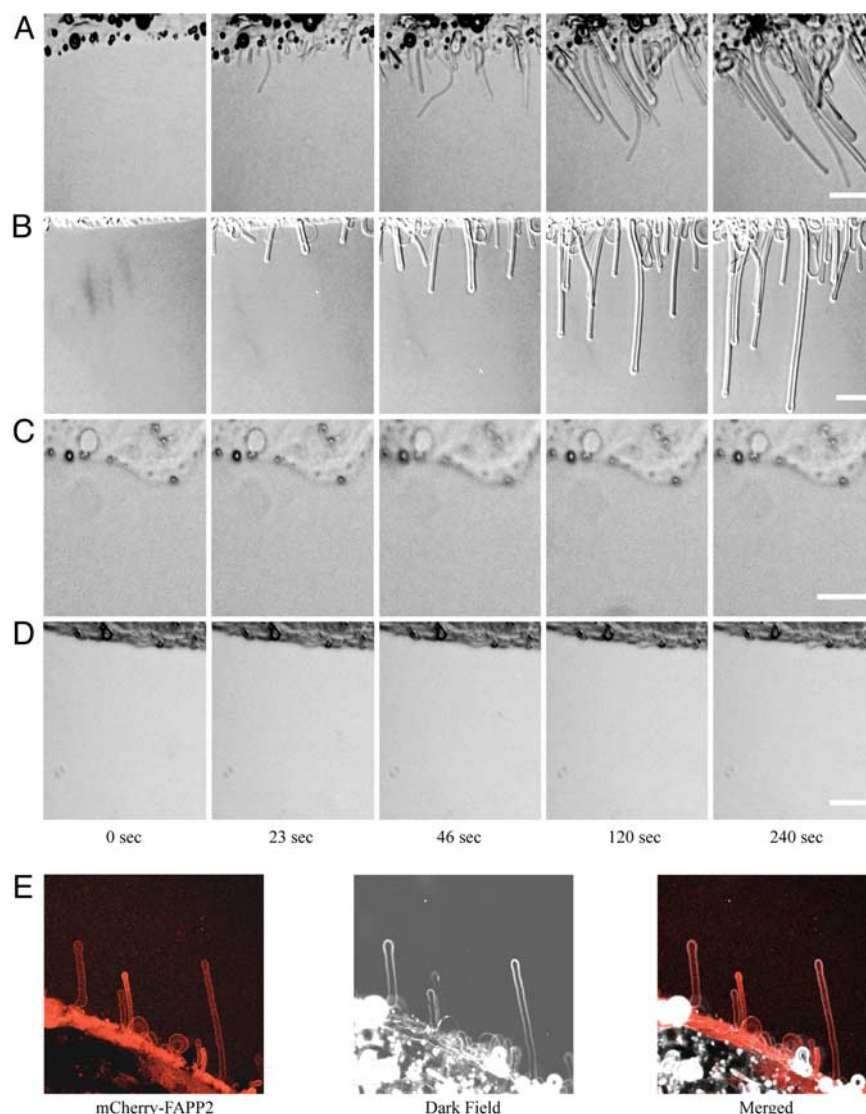


Fig. 1. FAPP2-mediated tubulation of flat membrane sheets. Tubulation activity of FAPP2 on membrane sheets with different compositions was followed by DIC. Lipids membrane sheets consisted of the following: (A) POPC:PI (4)P:GlcCer (96:2:2 mol%); (B) POPC:PI (4)P (98:2 mol%); (C) POPC; and (D) POPC:GlcCer (98:2 mol%). (E) Fluorescence and dark field images of tubules generated on membrane sheet containing POPC: PI (4)P (98:2 mol%) by mCherry-FAPP2. Tubulation was initiated by injection of 5 μ l FAPP2 (1 mg/ml) into the reaction chamber. Bars, 40 μ m.

consistent with our observation that GlcCer was not required for bilayer tubulation (Fig. 2C and [Movie S3](#)).

As an independent approach and also to measure the lipid-binding properties the FAPP2 protein, we measured the surface pressure changes ($\Delta\Pi$) on lipid monolayers containing POPC and PI (4)P (98:2 mol%) after continuous addition of FAPP2 ([Fig. S4](#)). For WT-FAPP2, a constant increase in pressure was noted up to 1.5 mN/m and at a protein concentration of 10 μ g/ml. At this point, surface pressure began to drop and reached a level well below the starting pressure value, indicating the removal of lipid by FAPP2. The FAPP2-R18L mutant, which is deficient in PI (4)P binding, behaved in the same way as the FAPP2 on POPC alone. FAPP2 associated linearly with the monolayer as the protein concentration was increased but caused no drop in pressure, indicating that although weak/transient binding did occur, no removal of lipids could be observed. Taken together, also here the FAPP2-PH domain appears to be required for membrane penetration and tubulation in vitro.

Solution State of FAPP2. A combined approach of analytical ultracentrifugation and chemical cross-linking was used to get

insights into the solution state of FAPP2. The ability of the GST protein to dimerize can influence the hydrodynamic properties of GST fusion proteins, complicating structural characterization. We therefore decided to produce an additional FAPP2 protein, which is tagged by 3myc and His₆ at the N- and C-termini. To define the relevant solution state of the FAPP2 proteins, size exclusion chromatography (SEC) and analytical ultracentrifugation (AUC) analysis of 3myc-FAPP2-His₆ and GST-FAPP2 were performed.

The SEC results revealed that the 3myc-FAPP2-His₆ protein eluted as one symmetric peak and was stable and monodispersed. The GST-FAPP2 protein formed additional, larger species, consistent with the ability of GST to dimerize ([Fig. S2A](#)). These states were stable in that they could be separated from each other over repeated SEC experiments to enrich for the main species. Both purified proteins were monodispersed based on sedimentation velocity centrifugation ([Fig. S3A](#)). The molecular weights were estimated from sedimentation equilibrium data, and showed that the 3myc-FAPP2-His₆ and GST-FAPP2 proteins were 129 and 166 kDa, respectively, over a broad

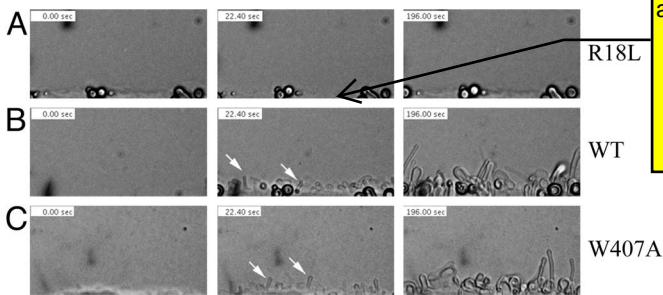


Fig. 2. Membrane tubulation activity of FAPP2 is PI (4)P dependent. Screen shots were taken from [Movies S1–S3](#). (A) PI (4)P binding–deficient FAPP2-R18L lacks tubulation activity, whereas addition of WT-FAPP2 rescues membrane tubulation (B). (C) FAPP2-W407A, lacking GlcCer binding, displays tubulation activity as WT-FAPP2. Fast and narrow tubules, indicated by arrows, are appearing at early time point as in Fig. 1A but grow back toward the lipid sheet. In all tubulation assays, a lipid mixture consisting of POPC:PI (4)P:GlcCer (96:2:2 mol%) was used. Tubulation was initiated by injection of 5 μ l FAPP2 (1 mg/ml) into the reaction chamber.

concentration range ([Table S2](#)). As the theoretical molecular mass of the respective monomers is 64 kDa and 84 kDa, the centrifugation data showed that both FAPP2 constructs are dimeric in solution. The dimeric state of each FAPP2 construct was confirmed by chemical cross-linking experiments using bis(sulfosuccinimidyl)-suberate (BS³). Both proteins yielded only one additional band on SDS/PAGE gradient gels with measured molecular weights of 159 and 205 kDa for 3myc-FAPP2-His₆ and GST-FAPP2, respectively, consistent with covalently modified dimeric states ([Fig. S3B](#)).

To account for any possible tag effects on the membrane tubulation activity, we also applied the 3myc-FAPP2-His₆ protein to our membrane sheet tubulation assay and could show that the membrane tubulation activity was retained ([Movie S4](#)).

Low-Resolution Structure of FAPP2. Given the novel membrane activity of FAPP2 and evidence of its dimeric solution state, we used SAXS to provide insights into the overall size, shape and

The GST-FAPP2 protein was not considered for analysis because of the bulky GST tag. Instead, a truncated version of FAPP2 (3mycFAPP2-His₆) was used. Inspection of the Guinier plots at low q and data quality and no protein aggregation. The pair distance distribution function $p(r)$ was calculated from the scattering intensities $I(s)$ using a reduced angular range from 0.07 nm^{-1} to 3 nm^{-1} , and the maximal particle size (D_{max}) was estimated to 30 nm ([Fig. 3B](#)). The radius of gyration (R_g) of 3myc-FAPP2-His₆ was found to be 8.37 nm. Together with the maximum molecular dimension of 30 nm, FAPP2 appears to be an extended protein assembly. This was also supported by the calculated prolate frictional ratio of 1.71, based on analytical ultracentrifugation data ([Table S2](#)). A low-resolution envelope model of FAPP2 was derived by ab initio shape modeling (see [Materials and Methods](#)). The molecular shape is a well extended and curved assembly. To assign the possible location of the FAPP2 protein domains, global rigid body modeling (see [Materials and Methods](#)) against the obtained scattering data indicated the GLTP and PH domain to be at either end of the dimeric FAPP2.

Discussion

Our data demonstrate that FAPP2 has the capability to form tubules from membrane sheets in vitro. This activity is dependent on the PI (4)P-binding activity of the PH domain of FAPP2. FAPP2 can thus be included in the growing list of proteins that can bend membranes to generate tubules.

Mechanism of Tubulation. Two principal mechanisms are used by proteins to induce membrane curvature. BAR domain-containing proteins are “banana-shaped” and thus confer curvature by direct membrane scaffolding (11–13). They bind to membranes by their positively charged concave face and therefore are able to sense, stabilize, and generate membrane curvature (14). The other mechanism relies on insertion of a small amphipathic or hydrophobic wedge to induce membrane asymmetry resulting in curvature (11, 15). These proteins include N-BAR domain-containing proteins having curvature-sensing

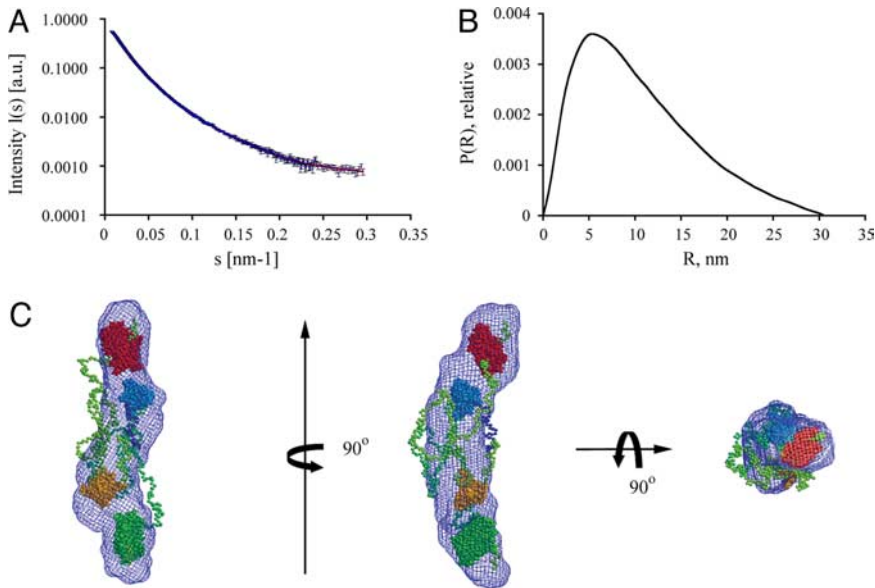


Fig. 3. SAXS analyses of dimeric 3myc-FAPP2-His₆ protein. (A) Experimental scattering curve (blue) and theoretical scattering curve of the modeled envelope structure (red). (B) Distance distribution function shows 3myc-FAPP2-His₆ to be an extended molecule \approx 30 nm in length. (C) Low-resolution envelope of 3myc-FAPP2-His₆ calculated by ab initio modeling (blue mesh surface). Rigid body modeling was used to calculate the possible locations of the PH- (blue and orange) proline-rich (light green) and GLTP (dark green and red) domain of FAPP2.

surfaces with additional N-terminally located amphipathic wedges, inbuilt to generate membrane deformation and tubulation. BAR and N-BAR domains can be extended additionally at their ends by lipid binding modules, such as PH and PX domains to localize the proteins at their intended compartment or by protein-protein interacting modules, like SH3 or PDZ domains. Our results suggest that FAPP2 also should be included in the growing repertoire of tubulating proteins. Stahelin et al. showed, in monolayer assays, that the FAPP1-PH domain also can penetrate into lipid monolayers and decrease the surface pressure (16). These data are in line with our monolayer assays and membrane sheet tubulation results. Altogether, these studies suggest that both membrane binding and tubulation is a property of the PH domain, which seems to be conserved in FAPP1 and FAPP2. The combined analytical centrifugation and SAXS analyses indicate an extended curved shape of the dimeric protein structure of 30 nm length. Because of the low resolution of the FAPP2 structure, it is unclear to what extent the curved shape of FAPP2 contributes to the described tubulation activity and/or to curvature-sensing activity.

FAPP2 in the Cell Biology Context. Whether FAPP2 exerts membrane tubulating activity in cells is not yet known. However, Godi et al. reported that in Cos7 cells overexpressing GST-tagged FAPP2, the protein is present on tubular extensions emanating from the TGN. We confirmed these results in MDCK cells. The carriers transporting protein cargo to the plasma membrane from the TGN are known to be pleiomorphic in shape, forming tubulovesicular structures and tubules of different lengths (17, 18). FAPP2 is also reported to bind the small GTPase, Arf1, another protein recently assigned a membrane-tubulating activity (19–21). It is possible that FAPP2 and Arf1 may act together, inducing membrane deformations leading to tubulation at the TGN. Our data demonstrate that the GLTP domain and its lipid target GlcCer do not play a direct role in the tubulation activity in vitro.

Thus the function of the GLTP domain in FAPP2 remains unclear. It could be involved in transferring GlcCer to the cellular site, where GlcCer can be translocated across the membrane to function as a precursor luminally for complex glycolipid synthesis either at the TGN or in the ER as suggested previously (7, 8). However, whether the membrane trafficking function could be explained solely by the glycolipid-transfer activity of FAPP2 seems unlikely because reduction of glycolipid biosynthesis has not previously been demonstrated to have such inhibitory effects on TGN to plasma membrane transport (22–24). It is also possible that FAPP2 functions as a sensor for regulating glycolipid levels in the cell. The presence of GlcCer on the cytoplasmic side of the TGN membrane could serve as a signal for FAPP2 to bind. It would do so by coincidence, binding to PI (4)P, Arf1, and potentially other factors. This ensemble would contribute to the formation and tubulation of transport carriers, which exit from the TGN to deliver both its protein and (glyco)lipid cargo to the cell surface. A feedback mechanism would limit GlcCer translocation from the cytosolic to the luminal leaflet when LacCer and other downstream glycolipids accumulate in the luminal leaflet of the TGN. Such a function would be in keeping with the proposition that lipid transfer

proteins in general could function as biosensors regulating lipid levels in the cell (24–26). Obviously this speculative hypothesis would need to be tested experimentally. Nevertheless the demonstration that FAPP2 has membrane tubulation activity brings in a new dimension in the mechanistic dissection of FAPP function in membrane trafficking.

Materials and Methods

In Vitro Tubulation of Flat Membrane Sheets. A system similar to that described in Roux et al. was used (9). Briefly, two 1- μ l droplets of a 10 mg/ml lipid stock solution with indicated composition (see *Results*) were spotted on each coverslip and allowed to dry. To remove any trace chloroform, lipid-coated coverslips were further dried under vacuum for at least 1 h. Lipids were then rehydrated for 20–30 min in an incubator (37 °C, 10% CO₂, and 100% humidity). A small reaction chamber was built by placing the coverslip over a glass slide with strips of double-sided tape as spacers. Subsequently, lipids were fully rehydrated by injecting 15–20 μ l buffer (20 mM Hepes-NaOH, pH 7.4, 100 mM NaCl, 1 mM MgCl₂, 1 mM DTT), containing 0.1 mg/ml casein (C7078, Sigma) into the chamber. A 5- μ l quantity of protein solution (1 mg/ml) was then injected and the deformation of membrane sheets was recorded by DIC microscopy on a Zeiss Axioplan 2 microscope (Carl Zeiss Jena) equipped with EC Plan-Neofluar 10x/0.3 objective.

X-Ray Scattering Experiments and Data Analysis. SAXS data were collected at the updated X33 beamline (27–29) using a MAR345 image plate detector (MarResearch, Norderstedt, Germany) located at the EMBL Hamburg Outstation located on a bending magnet (sector D) on the storage ring DORIS III of the Deutsches Elektronen Synchrotron (DESY). A single photon counting pixel detector system (PILATUS 500k) was used as detector. A sample-detector distance of 2,675 mm was used, covering the range of momentum transfer $0.1 < s < 5 \text{ nm}^{-1}$ ($s = 4\pi \sin(\theta)/\lambda$, where θ is the scattering angle and $\lambda = 0.1504 \text{ nm}$ is the x-ray wavelength). The s-axis was calibrated by the scattering pattern of Silver-behenate salt (*d*-spacing 5.84 nm). The scattering patterns from 3myc-FAPP2-His protein was measured at protein concentrations of 3.87 and 7.74 mg/ml. Protein sample was prepared in Dulbecco's PBS and 20 mM DTT as radical quencher. Four repetitive measurements of 30 s at 15 °C of the same protein solution were performed to check for radiation damage. All initial data treatment was performed with the program PRIMUS (30), including estimation of the radius of gyration and the maximal dimension of the protein after Fourier transformation of the scattering intensity.

For the initial shape analysis, 20 independent ab initio calculations using the program DAMMIN (31) were performed. A dimeric symmetry constraint was applied, and χ^2 values obtained by this standard procedure ranged from 1.3 to 1.7. The resulting low-resolution envelope models were averaged accounting for the ambiguity of solution scattering methods. Low NSD variations indicate high structural similarity of these models, and a total of 18 models were used for the averaging.

A more elaborated analysis method is used by program BUNCH (32). Based on a homology model of the PH domain and the x-ray structure of the human GLTP protein (PDB 1swx), a structural model for the entire protein was derived. Here also the dimeric constraint was applied. To account for the lack of high-resolution information the proline-rich domain was modeled as random chain amino acids. The best-fit model was obtained by additional constraints were chain interactions in the proline-rich domain between 260 and 280 were defined, decreasing the number of orientations of the flexible random chain amino acids. Here also 20 independent BUNCH runs were performed.

ACKNOWLEDGMENTS. We thank Rosemary Parslow (School of Biological Sciences, Birmingham, UK) for skillful handling of the analytical ultracentrifugation runs; the entire Simons laboratory for helpful and encouraging discussions; and Gerhard Grüber (School of Biological Sciences, NTU Singapore) for his kind offer to share beam-time at the EMBL Hamburg-Outstation. This work was supported by grants from Deutsche Forschungsgemeinschaft (SFB/TR13–04 and SP1175) (to K.S.) and the EU FP6 “PRISM” project (to M.O. and K.S.).

1. Fölsch H (2008) Regulation of membrane trafficking in polarized epithelial cells. *Curr Opin Cell Biol* 20:208–213.
2. Schuck S, Simons K (2004) Polarized sorting in epithelial cells: Raft clustering and the biogenesis of the apical membrane. *J Cell Sci* 117:5955–5964.
3. Rodriguez-Boulant E, Kreitzer G, Musch A (2005) Organization of vesicular trafficking in epithelia. *Nat Rev Mol Cell Biol* 6:233–247.
4. Godi A, et al. (2004) FAPPs control Golgi-to-cell-surface membrane traffic by binding to ARF and PtdIns(4)P. *Nat Cell Biol* 6:393–404.
5. Vieira OV, Verkade P, Manninen A, Simons K (2005) FAPP2 is involved in the transport of apical cargo in polarized MDCK cells. *J Cell Biol* 170:521–526.

6. Yui N, et al. (2009) FAPP2 is required for aquaporin-2 apical sorting at trans-Golgi network in polarized MDCK cells. *Am J Physiol Cell Physiol*.
7. D'Angelo G, et al. (2007) Glycosphingolipid synthesis requires FAPP2 transfer of glucosylceramide. *Nature* 449:62–67.
8. Halter D, et al. (2007) Pre- and post-Golgi translocation of glucosylceramide in glycosphingolipid synthesis. *J Cell Biol* 179:101–115.
9. Roux A, Uyhazi K, Frost A, De Camilli P (2006) GTP-dependent twisting of dynamin implicates constriction and tension in membrane fission. *Nature* 441:528–531.
10. Dowler S, et al. (2000) Identification of pleckstrin-homology-domain-containing proteins with novel phosphoinositide-binding specificities. *Biochem J* 351:19–31.

AQ: G

AQ: F

11. McMahon HT, Gallop JL (2005) Membrane curvature and mechanisms of dynamic cell membrane remodelling. *Nature* 438:590–596.
12. Farsad K, De Camilli P (2003) Mechanisms of membrane deformation. *Curr Opin Cell Biol* 15:372–381.
13. Zimmerberg J, Kozlov MM (2006) How proteins produce cellular membrane curvature. *Nat Rev Mol Cell Biol* 7:9–19.
14. Peter BJ, et al. (2004) BAR domains as sensors of membrane curvature: The amphiphysin BAR structure. *Science* 303:495–499.
15. Blood PD, Voth GA (2006) Direct observation of Bin/amphiphysin/Rvs (BAR) domain-induced membrane curvature by means of molecular dynamics simulations. *Proc Natl Acad Sci USA* 103:15068–15072.
16. Stahelin RV, Karathanassis D, Murray D, Williams RL, Cho W (2007) Structural and membrane binding analysis of the Phox homology domain of Bem1p: Basis of phosphatidylinositol 4-phosphate specificity. *J Biol Chem* 282:25737–25747.
17. Lippincott-Schwartz J, Liu W (2003) Membrane trafficking: Coat control by curvature. *Nature* 426:507–508.
18. Keller P, Simons K (1997) Post-Golgi biosynthetic trafficking. *J Cell Sci* 110:3001–3009.
19. Lundmark R, Doherty GJ, Vallis Y, Peter BJ, McMahon HT (2008) Arf family GTP loading is activated by, and generates, positive membrane curvature. *Biochem J* 414:189–194.
20. Beck R, et al. (2008) Membrane curvature induced by Arf1-GTP is essential for vesicle formation. *Proc Natl Acad Sci USA* 105:11731–11736.
21. Krauss M, et al. (2008) Arf1-GTP-induced tubule formation suggests a function of Arf family proteins in curvature acquisition at sites of vesicle budding. *J Biol Chem* 283:27717–27723.
22. Degroote S, Wolthoorn J, van Meer G (2004) The cell biology of glycosphingolipids. *Semin Cell Dev Biol* 15:375–387.
23. Tamboli IY, et al. (2005) Inhibition of glycosphingolipid biosynthesis reduces secretion of the beta-amyloid precursor protein and amyloid beta-peptide. *J Biol Chem* 280:28110–28117.
24. D'Angelo G, Vicinanza M, De Matteis MA (2008) Lipid-transfer proteins in biosynthetic pathways. *Curr Opin Cell Biol* 20:360–370.
25. Bankaitis VA, et al. (2005) Phosphatidylinositol transfer protein function in the yeast *Saccharomyces cerevisiae*. *Adv Enzyme Regul* 45:155–170.
26. Mattjus P (2009) Glycolipid transfer proteins and membrane interaction. *Biochim Biophys Acta* 1788:267–272.
27. Koch MHJ, Bording J (1983) X-ray diffraction and scattering on disordered systems using synchrotron radiation. *Nucl Instrum Methods Phys Res* 208:461–469.
28. Roessle MW, et al. (2007) Upgrade of the small-angle X-ray scattering beamline X33 at the European Molecular Biology Laboratory, Hamburg. *J Appl Crystallogr* 40:190–194.
29. Round AR, et al. (2008) Automated sample-changing robot for solution scattering experiments at the EMBL Hamburg SAXS station X33. *J Appl Crystallogr* 41:913–917.
30. Konarev PV, Volkov VV, Sokolova AV, Koch MHJ, Svergun DI (2003) PRIMUS: A Windows PC-based system for small-angle scattering data analysis. *J Appl Crystallogr* 36:1277–1282.
31. Svergun DI (1999) Restoring low resolution structure of biological macromolecules from solution scattering using simulated annealing. *Biophys J* 76:2879–2886.
32. Petoukhov MV, Svergun DI (2005) Global rigid body modeling of macromolecular complexes against small-angle scattering data. *Biophys J* 89:1237–1250.

PNAS proof
Embargoed

Supporting Information

Cao et al. 10.1073/pnas.0911789106

SI Materials and Methods

Reagents. Chemical cross-linker BS3 was from Pierce/Thermo Scientific. Ni²⁺-NTA Superflow was supplied by Qiagen, and Glutathione Sepharose 4B as well as Superdex 200 HR 10/30 by GE Healthcare Europe GmbH.

Cloning of FAPP2 and Plasmid Construction. Total RNA was isolated from Madin-Darby canine kidney II (MDCK II) cells using RNAeasy Qiagen kit. RT-PCR was performed using SuperScript reverse transcriptase (Invitrogen) with a poly dT oligo as primer. The cDNA was used as template for PCR. According to FAPP2 sequence predicted by Bioinformatics (provided by MPI-CBG Bioinformatics Facility), primers for FAPP2 were designed as following: forward primer 5'-ATG GAG GGG GTG CTG TAC AAG T-3' and reverse primer 5'-TAC CAC CTC ATC AGA CTC CAG-3'. The PCR products were cloned into pCR4-TOPO vector using TOPO TA Cloning kit (Invitrogen), and processed for sequencing. FAPP2 was then cloned into site SalI/NotI of pET-24d (Novagen), which was modified with a 3myc-tag at the N terminus, or into the EcoRI/SalI site of pGEX-6P-1 (GE Healthcare). For the construction of mCherry-FAPP2, FAPP2 was inserted into the SalI/XhoI site of a modified pGEX-6P-1, in which mCherry was in frame with the EcoRI/SalI inserted mCherry. GST-tagged FAPP2 mutants R18L, W407A were created using the QuikChange XL site-directed mutagenesis kit (Stratagene, La Jolla, CA) according to the manufacturer's manual using primers as described in Table S1. All constructs were sequenced in full.

Protein Expression and Purification. Transfected BL 21(DE3) cells were grown in LB medium at 37 °C, induced with 0.1 mM isopropyl-β-D-thiogalactopyranoside (IPTG), and grown for another 16–20 h at 18 °C. Purification of recombinant proteins from *E. coli* lysate protein was accomplished by Ni²⁺ and glutathione affinity chromatography, respectively, following the manufacturer's instructions. PBS containing 9.6 mM β-mercaptoethanol was used for all purification steps. For the elution of His-tagged protein, an imidazole step gradient (40 mM, 60 mM, 80 mM, 100 mM, 120 mM, and 200 mM) in elution buffer was applied with five column volumes in each step. Fractions containing FAPP2 were pooled and subsequently applied on a Superdex 200 HR 10/300 column (GE Healthcare) equilibrated in PBS with 9.6 mM β-mercaptoethanol. Protein containing fractions were pooled and concentrated by ultrafiltration in YM-100 units (Millipore). In case of GST-FAPP2, the size exclusion chromatography was optionally performed.

Lentivirus Production. EGFP-FAPP2 was cloned into the lentiviral pRRLSIN. cPPT. SFFV/GFP. WRPR (provided by Marino Zerial) using the restriction sites BamHI and SalI. The intrinsic GFP fusogenic site of the aforementioned lentiviral vector was removed through this insertion. The construct was further transfected into HEK 293T cells using helper plasmids pVSVG, pSPAX2 and Lipofectamine 2000 transfection reagent (Invitrogen). After 48 h of infection, supernatants bearing lentiviral particles were used to infect MDCK II epithelial cells. EGFP-FAPP2 expression was visible in 3 days, and the maximum expression was achieved within 5–6 days.

Immunostaining and Confocal Microscopy. Wild-type and TGN38-myc stable MDCK II cell lines were grown over night on coverslips, fixed, and immunostained as described elsewhere (1). Images were analyzed using LSM-510 META laser scanning confocal microscope with a plan-Apochromat 100x immersion oil objective (Carl Zeiss Jena). The antibodies were used in following dilutions: rabbit anti-furin (Affinity Bioreagents) 1:500, mouse anti-FAPP2 (clone A655-A08-2, prepared by the Antibody Facility, MPI-CBG Dresden) 1:100 and rabbit anti-myc (Santa Cruz) 1:500.

Surface Pressure Measurements of Lipid Monolayers. Monolayer tests were performed via the surface pressure measurement by the Wilhelmy plate (Whatman Chr1), using a trough with a constant surface area 24 cm² (volume 35 ml) and a Nima tensiometer (Nima Technology) at room temperature. The monolayer was formed in a dropwise manner by the injection of a chloroform solution of a mixture of POPC:PI (4)P 98:2 mol% (1 mg/ml) onto the subphase. The measurements were performed after evaporation of the organic solvent (15 min), at an initial surface pressure of 30 mN/m (± 1 mN/m). WT-FAPP2 was dialyzed against assay buffer (25 mM Hepes, pH 7.25, 150 mM NaCl, 9.6 mM β-mercaptoethanol) and injected into the subphase to obtain the indicated concentration. The changes in the surface pressure were recorded after the system reached equilibrium (usually after 3 min). The protein concentration in the subphase was increased by stepwise injection after 5 min. As a control the respective volume of buffer was injected into the subphase.

Analytical Ultracentrifugation. A Beckman XL-I analytical ultracentrifuge (Beckman Coulter) using an eight-cell 50Ti rotor was used for the analytical ultracentrifugation studies. For both velocity and equilibrium sedimentation experiments, samples of FAPP2 protein were prepared in Dulbecco's PBS including 9.6 mM β-mercaptoethanol. Sedimentation velocity experiments were carried out by centrifuging a two-sector cell at 40,000 rpm for 17 h at 4 °C. The absorbance of the sample was measured at a wavelength of 280 nm throughout the cell. A total of 126 measurements were taken of each sample during the run. These data were then analyzed by applying the c(s) routine in SEDFIT (2), with values for the partial specific volume of the protein, viscosity, and density of the buffer being calculated using SEDNTERP (3). The resulting values were then converted to S_{20,w} using SEDNTERP.

Sedimentation equilibrium experiments were carried out by centrifuging a six-sector cell at 8,000, 11,000, and 14,000 rpm at 4 °C. Each speed was maintained for 20 h, and readings were then taken once per hour for the next 4 h. These scans were then compared to ensure that the sample had reached equilibrium. These data were analyzed using SEDPHAT (4), applying a single-species model with mass free to vary for the 3myc-FAPP2-His₆ and a two-species model with mass free to vary for the GST-FAPP2. The latter model was used to take into account a low-molecular-weight contaminant <1000 Da that made fitting with a single species model impossible. The prolate frictional ratios [*f*/*f*_p] for both FAPP2 constructs were calculated using SEDNTERP.

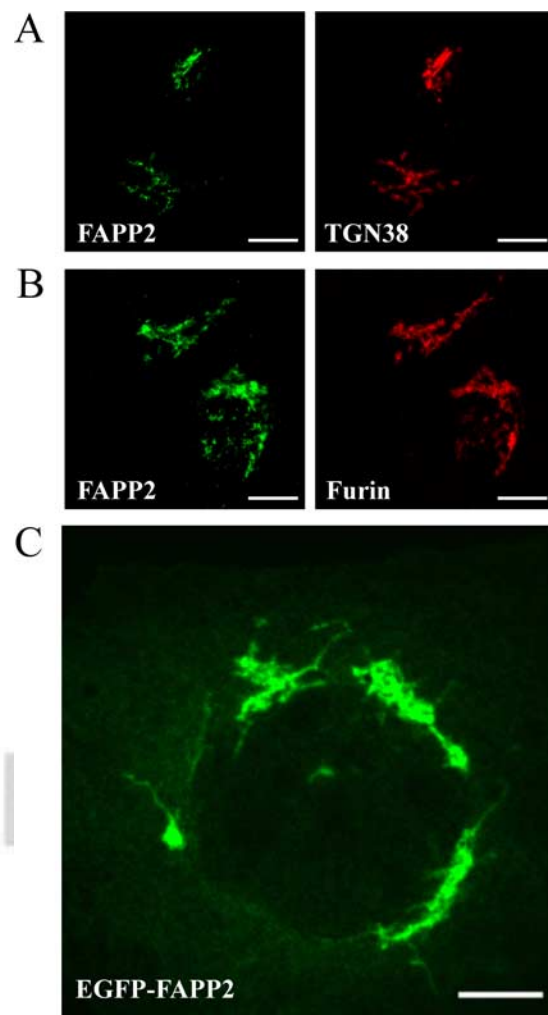


Fig. S1. Localization of FAPP2 at the TGN and its tubules. TGN38-myc stable cells were double-labeled with monoclonal A655-A08-2 anti-FAPP2 (green) and rabbit anti-myc (red) (A) and rabbit anti-furin (B) antibodies. (Scale bar, 10 μ m.) (C) EGFP-FAPP2 lentiviral overexpression induced Golgi tubulation. (Scale bar, 5 μ m.)

SF1

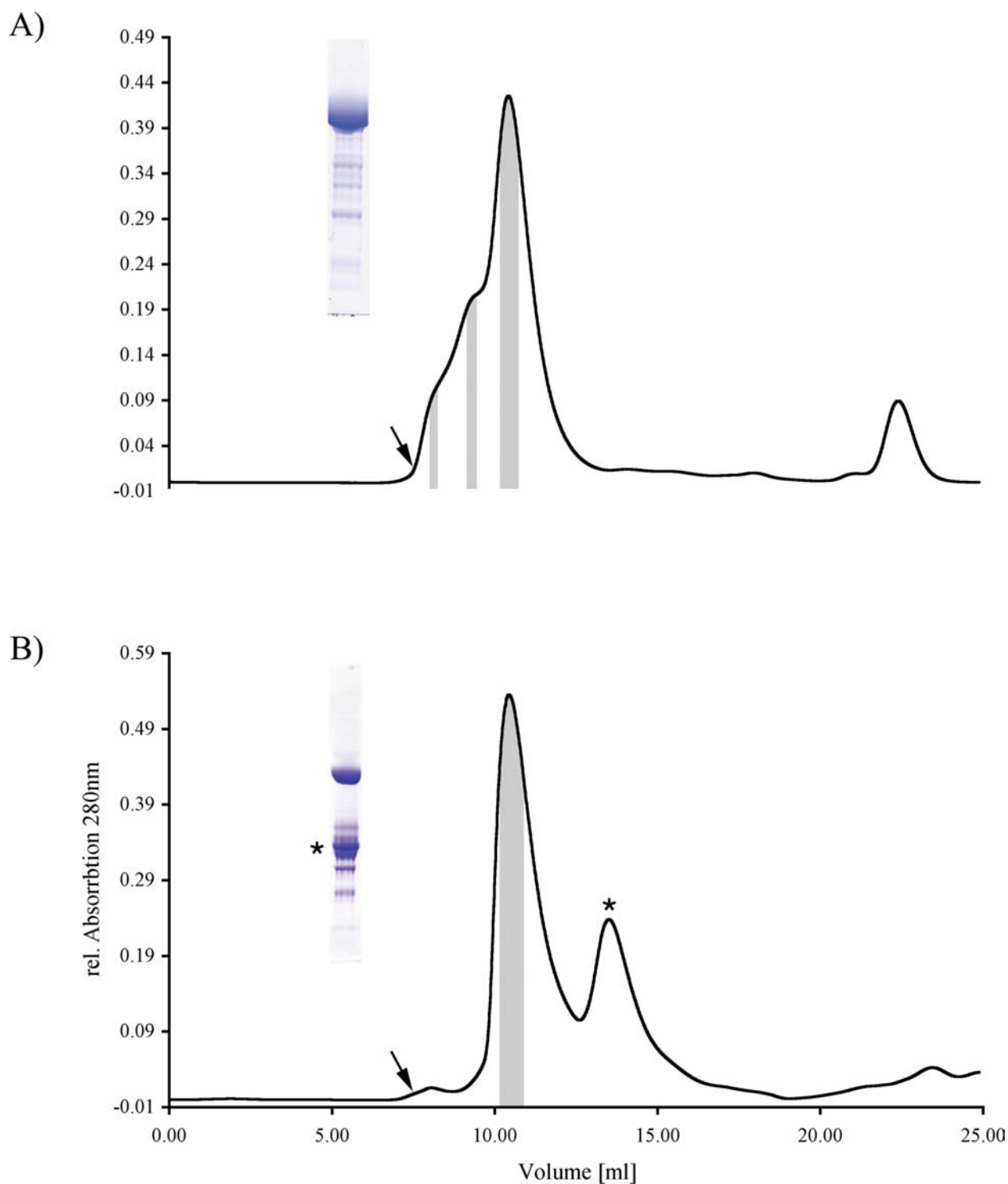


Fig. S2. Size exclusion chromatography profiles. Affinity purified proteins were loaded on Superdex-200 HR10/30 column after equilibrating with PBS and 9.6 mM β -mercaptoethanol. SDS/PAGE of GST-FAPP2 (A) or 3myc-FAPP2-His₆ (B) protein samples before SEC is depicted in *insets*. FAPP2 containing fractions are indicated by gray-shaded areas. For biochemical and structural experiments, only fractions after a retention volume of ≈ 10 ml were used. The GST-FAPP2 protein eluted as polydispersed protein indicated by additional shoulders at early retention volumes, whereas 3myc-FAPP2-His₆ eluted in a single peak. Second peak in the 3myc-FAPP2-His₆ profile represents low-molecular-weight impurities, labeled with asterisk. Black arrows indicate the column void volume. For SDS/PAGE of the purified proteins after SEC, see Fig. S3.

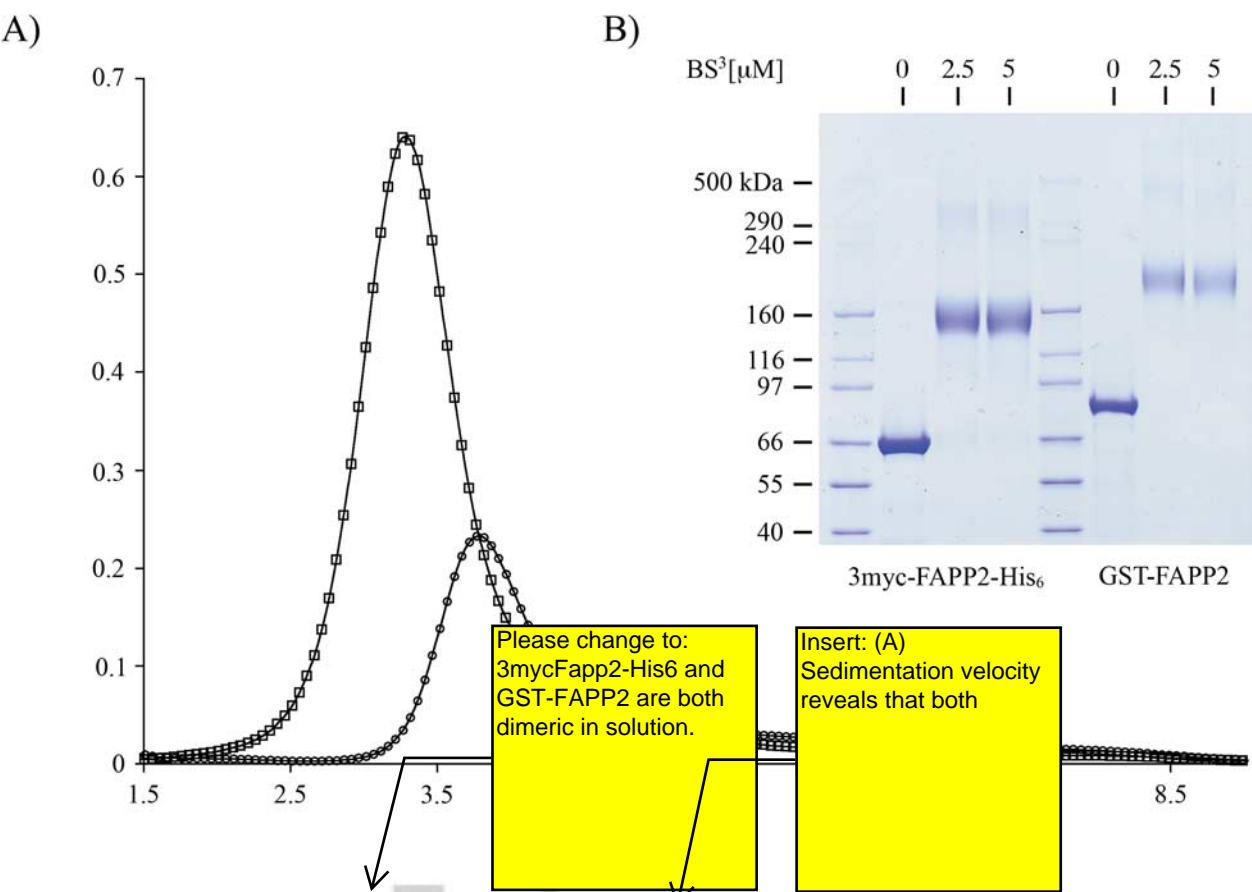


Fig. S3. Sedimentation velocity centrifugation of 3myc-FAPP2-His and GST-FAPP2. Both proteins are monodispersed in solution with S values of 3.31(3myc-FAPP2-His₆, squares) and 3.84 (GST-FAPP2, circles) respectively (see [SI Materials and Methods](#)). (B) GST-FAPP2 and 3myc-FAPP2-His₆ were incubated with the chemical cross-linker BS³ at indicated concentrations at room temperature for 30 min. Cross-linking products were resolved on 3–8% NuPAGE Tris-Acetate Gradient gels.

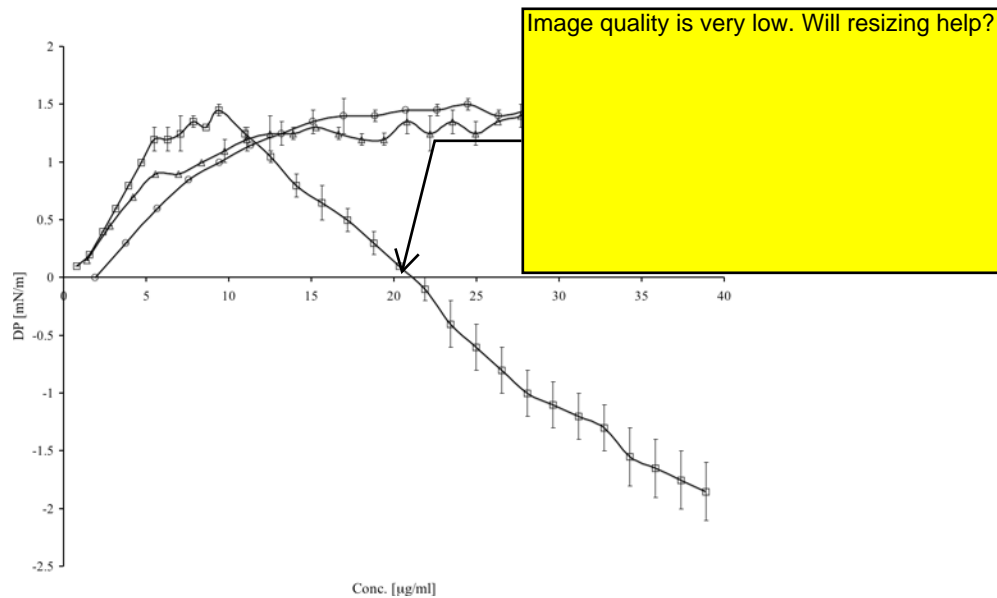
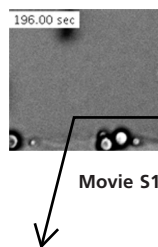


Fig. S4. FAPP2 removes lipids on a monolayer lipid surface. Surface pressure changes ($\Delta\Pi$) after injection of WT-FAPP2 and mutants in the subphase of POPC and PI (4)P (98:2 mol%) lipid monolayers. Isotherm was normalized to the initial established Π (≈ 3 mN/m).

SF4

PNAS proof
Embargoed

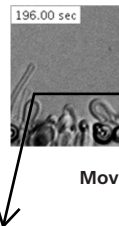


Legend: The PH domain of FAPP2 is involved in tubulation. FAPP2-R18L is a tubulation deficient FAPP2-R18L lacks tubulation activity. Lipid mixture PI(4)P:GlcCer (96:2:2 mol%). Tubulation was initiated by in (1mg/ml) into the reaction chamber.

AQ: M

ZSM1.mov [Movie S1](#)

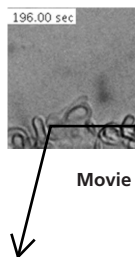
PNAS proof
Embargoed



Legend: Addition of WT-FAPP2 into the same reaction chamber
tubulation

PNAS proof
Embargoed

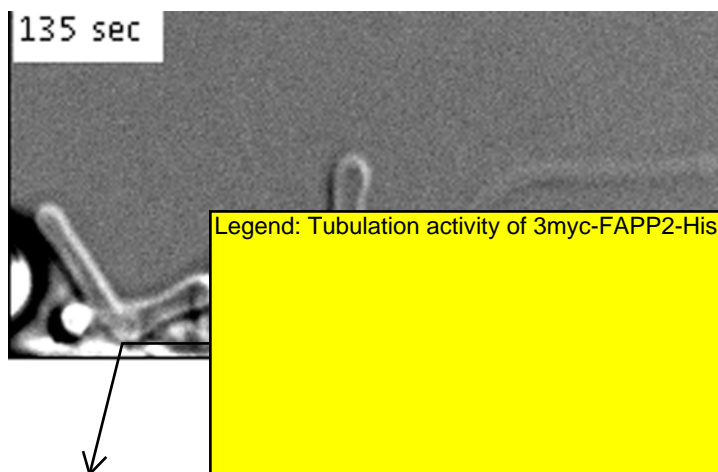
ZSM2.mov [Movie S2](#)



Legend: The glycolipid binding domain GLTP is no involved i
tubules. FAPP2-W407A, lacking GlcCer binding, displays tub

ZSM3.mov [Movie S3](#)

PNAS proof
Embargoed



ZSM4.moy [Movie S4](#)

PNAS proof
Embargoed

Table S1. Primers for GST-FAPP2 mutants

Mutant	Primer
R18L	Forward 5'- CTG AGC GGT TGG CAG CCT CTA TGG TTC CTA CTC TG –3' Reverse 5'- CAG AGT AGG AAC CAT AGA GGC TGC CAA CCG CTC AG –3'
W407A	Forward 5'- GCT ACA GAA GCC CTC TTG GCG CTG AAG AGA GGT CTC –3'

PNAS proof
Embargoed

Table S2. Analytical ultracentrifugation results

	3myc-FAPP2-His ₆	GST-FAPP2
S	3.31 ± 0.258	3.84 ± 0.184
S ^o _{20,w}	5.25	5.97
MW from equilibrium	129 kDa ± 1.6	166 kDa ± 3.3
Prolate frictional ratio (<i>f/f_p</i>)	1.71	1.76

ST2

PNAS proof
Embargoed

AUTHOR QUERIES

AUTHOR PLEASE ANSWER ALL QUERIES

1

- A—Please contact Betty Cherniak at **PNASProofReturn@cadmus.com**. or 410-691-6452 if you have questions about the editorial changes, this list of queries, or the figures in your article. **Please include your manuscript number in all e-mail correspondence (the number begins with 08 or 09 and is followed by five additional numbers, e.g., 08-01234).** Furthermore, if returning proofs electronically, please e-mail them to the above address. Please (i) review the author affiliation and footnote symbols carefully, (ii) check the order of the author names, and (iii) check the spelling of all author names and affiliations. Please indicate that the author and affiliation lines are correct by writing 'OK' in the margin next to the author line. Please note that this is your opportunity to correct errors in your article prior to publication. **Corrections requested after online publication will be considered and processed as errata.**
- B—PNAS does not allow statements of novelty or priority. Please rewrite/approve edit.
- C—Au: The key term 'FAPP2' has been deleted because it appears in the title, which is searchable on line. You may add 1 key term that does not appear in the title and is not a nonstandard abbreviation.
- D—Please verify that all supporting information (SI) citations are correct. Note, however, that the hyperlinks for SI citations will not work until the article is published online. In addition, SI that is not composed in the main SI PDF (appendices, datasets, movies, and 'Other Supporting Information Files') have not been changed from your originally submitted file and so are not included in this set of proofs. The proofs for any composed portion of your SI are included in this proof as subsequent pages following the last page of the main text. If you did not receive the proofs for your SI, please contact PNASproofreturn@cadmus.com.
- E—Au: If your article contains figures that were submitted in an unsupported or problematic format (e.g., any format other than .eps or .tif), please check the quality of the figures closely. Please note that if figures need to be replaced, the standard charges listed on the reprint form may be incurred.
- F—Au: Please ensure that first five authors are listed before 'et al.' in all references in which 'et al.' is used.
- G—Au: Please provide journal volume and article page range.
- H—Please review the information in the author contribution footnote carefully. Please make sure

AUTHOR QUERIES

AUTHOR PLEASE ANSWER ALL QUERIES

2

that the information is correct and that the correct author initials are listed. Note that the order of author initials matches the order of the author line per journal style. You may add contributions to the list in the footnote; however, funding should not be an author's only contribution to the work.

I—Au: Please review the information in the author contribution footnote carefully. Please make sure that the information is correct and that the correct author initials are listed. Note that the order of author initials matches the order of the author line per journal style. You may add contributions to the list in the footnote; however, funding should not be an author's only contribution to the work.

J—Au: Reminder: You have chosen not to pay an additional \$1200 (or \$850 if your institution has a site license) for the PNAS Open Access option.

K—Au: Each corresponding author is required to return a completed Reprint and Publication Charges form, whether or not reprints are ordered. Please complete the form, including payment information for applicable publication charges (purchase order number or credit card information), and return the form with your proof corrections. Failure to return a completed form may result in publication delays.

L—Au: Please precede description of (*B*) with description of (*A*), either individually or in combination with (*B*).

M—Au: Please supply legends for Movies 1–4.

Instructions for Annotating Your .PDF Proof

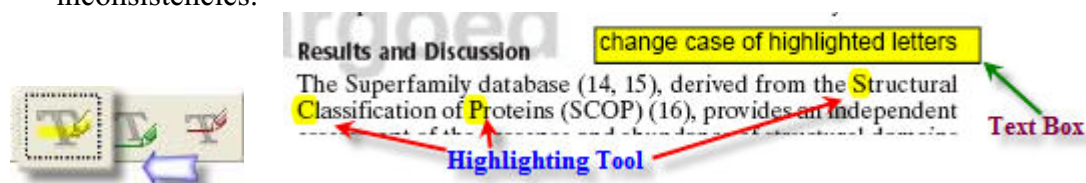
- Use Text Boxes and the Callout Tool to indicate changes to the text.



- Use the Strike-Out tool to indicate deletions to the text.



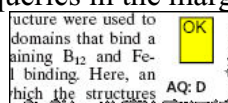
- Use the Highlighting Tool to indicate font problems, bad breaks, and other textual inconsistencies.



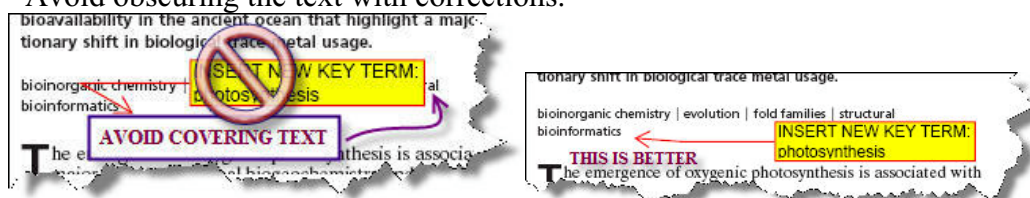
- Clearly indicate where changes need to be made using arrow, lines, and the Call-Out Tool.



- Mark changes and answer queries in the margins and other areas of white space.



- Avoid obscuring the text with corrections.



Proofreader's Marks

MARK	EXPLANATION	EXAMPLE
	TAKE OUT CHARACTER INDICATED	 Your proof.
^	LEFT OUT, INSERT	u Your proof. ^
#	INSERT SPACE	# Your proof. ^
9	TURN INVERTED LETTER	Your p ⁹ roof. ^
X	BROKEN LETTER	X Your pr ^X oof.
eq#	EVEN SPACE	eq# A good proof.
○	CLOSE UP: NO SPACE	Your pro [○] gf.
tr	TRANSPOSE	tr A ^{tr} proofgood
wf	WRONG FONT	wf Your pro ^{wf} of.
lc	LOWER CASE	lc Your ^{lc} proof.
≡	CAPITALS	Your proof. caps <u>Y</u> our proof.
ital	ITALIC	Your proof. ital <u>Y</u> our proof.
rom	ROMAN, NON ITALIC	rom Your <u>proof</u> .
bf	BOLD FACE	Your proof. bf <u>Y</u> our proof.
..... stet	LET IT STAND	Your proof. stet Your proof.
out sc.	DELETE, SEE COPY	out sc. She ^{out sc.} Our proof.
spell out	SPELL OUT	spell out Queen (Eliz.)
¶	START PARAGRAPH	¶ read. [Your
no ¶	NO PARAGRAPH: RUN IN	no ¶ marked. → ¶ Your proof.
└	LOWER	└ [Your proof.]

MARK	EXPLANATION	EXAMPLE
┐	RAISE	┐ [Your proof.]
└	MOVE LEFT	└ Your proof.
┘	MOVE RIGHT	┘ Your proof.
	ALIGN TYPE	└ Three dogs. Two horses.
==	STRAIGHTEN LINE	= Your <u>proof</u> .
⊙	INSERT PERIOD	⊙ Your proof [^]
;/	INSERT COMMA	;/ Your proof [^]
:/	INSERT COLON	:/ Your proof [^]
;/	INSERT SEMICOLON	;/ Your proof [^]
∨	INSERT APOSTROPHE	∨ Your m [∨] ans proof. ^
∨ ∨	INSERT QUOTATION MARKS	∨ ∨ Marked it proof [^]
=/	INSERT HYPHEN	=/ A proof [^] mark.
!	INSERT EXCLAMATION MARK	! Prove it [^]
?	INSERT QUESTION MARK	? Is it right [^]
②	QUERY FOR AUTHOR	② was Your proof [^] read by
[/]	INSERT BRACKETS	[/] The Smith [^] girl [^]
(< />)	INSERT PARENTHESES	(< />) Your proof [^] 1 [^]
1/m	INSERT 1-EM DASH	1/m Your proof. [^]
□	INDENT 1 EM	□ Your proof
▢	INDENT 2 EMS	▢ Your proof.
▣	INDENT 3 EMS	▣ Your proof.

2009 Reprint and Publication Charges

Reprint orders and prepayments must be received no later than 2 weeks after return of your page proofs.

PUBLICATION FEES

Page Charges

(Research Articles Only)

Page charges of \$70 per journal page are requested for each page in the article. PNAS charges for extensive author alterations on proofs. Six or more author alterations per page will be charged at \$4 each. Authors will not be charged for correcting printer's errors, copyediting errors, or figure errors made in composition.

Articles Published with Figures

(Research Articles Only)

If your article contains color, add \$300 for each color figure or table. Replacing, deleting, or resizing color will cost \$150 per figure or table. Replacing black-and-white figures will cost \$25 per figure. Replacing supporting information figures will cost \$25 per figure. State the exact figure charge on the following page and add to your payment or purchase order accordingly.

Supporting Information (SI)

(Research Articles Only)

SI for the web will cost \$250 per article. Four or more author alterations per SI page will be charged at \$4 each.

PNAS Open Access Option

Authors may pay a surcharge of \$1200 to make their paper freely available online immediately upon publication. If your institution has a 2009 Site License, the open access surcharge is \$850. If you wish to choose this option, please notify the Editorial Office (pnas@nas.edu) immediately, if you have not already done so.

Shipping

UPS ground shipping within the continental US (1–5 days delivery) is included in the reprint prices, except for orders over 1,000 copies. Orders are shipped to authors outside the continental US via expedited delivery service (included in the reprint prices).

Multiple Shipments

You may request that your order be shipped to more than one location. Please add \$45 for each additional address.

Delivery

Your order will be shipped within 2 weeks of the journal publication date.

Tax Due

For orders shipped to the following locations, please add the appropriate sales tax: Canada – 5%; in the US: CA – 8.25% plus the city and county rate; CT – 6%; DC – 6%; FL – 6% sales tax plus local surtax, if you are in a taxing county; MD – 6%; NC – 4.5%; NY – state and local sales taxes apply; VA – 5%; WI – 5%. A copy of the state sales tax exemption certificate must accompany the order form; otherwise sales tax will be assessed (billed).

Ordering

Prepayment or a signed institutional purchase order is required to process your order. You may use the following page as a Proforma Invoice. Please return your order form, purchase order, and payment to:

PNAS Reprints

PO Box 631694
Baltimore, MD 21263-1694
FEIN 53-0196932

Please contact June Billman by e-mail at billmanj@cadmus.com, phone 1-866-HURLOCK (toll free) or 1-410-943-3086, or fax 1-877-705-1373 if you have any questions.

Covers are an additional \$85 regardless of the reprint quantity ordered. Please see reprint rates and cover image samples below.

Rates for Black-and-White Reprints* (Minimum order 50. Includes shipping.)

Quantity	50	100	200	300	400	500	Add'l 50s over 500
Domestic	\$485	\$655	\$680	\$745	\$800	\$850	\$60
Foreign	\$525	\$695	\$755	\$850	\$935	\$1,010	\$85

* Color covers may be ordered for black-and-white reprints; however, color reprint rates (below) will apply.

For Black-and-White and Color Reprint Covers add \$85

Rates for Color Reprints† (Minimum order 50. Includes shipping.)

Quantity	50	100	200	300	400	500	Add'l 50s over 500
Domestic	\$545	\$675	\$910	\$1,220	\$1,570	\$1,915	\$175
Foreign	\$605	\$730	\$975	\$1,320	\$1,730	\$2,220	\$240

†Please return your order form promptly.



Covers for black-and-white reprints will display the volume, issue, page numbers, and black-and-white PNAS masthead with the reprint article title and authors imprinted in the center of the page.‡



Covers for color reprints will display the volume, issue, page numbers, and the color PNAS masthead and will include the issue cover image with the reprint article title and authors imprinted in the center of the page.‡

‡Covers for all reprints will be printed on the same paper stock as the article.

2009 Reprint Order Form or Proforma Invoice

(Please keep a copy of this document for your records.)

Reprint orders and payments must be received no later than 2 weeks after return of your proofs.**1 Publication Details**Reprint Order Number 3545220

Author's Name _____

Title of Article _____

Number of Pages _____ Manuscript Number 09-11789Are there color figures in the article? ☐ Yes ☐ No**2 Reprint Charges (Use Rates Listed on Previous Page)**

Indicate the number of reprints ordered and the total due. Minimum order is 50 copies; prices include shipping.

Research, Special Feature Research, From the Academy, and Colloquium Articles:

_____ Reprints (black/white only) \$ _____

_____ Color Reprints (with or without color figures) \$ _____

_____ Covers \$ _____

For Commentary, Inaugural, Solicited Review, and Solicited Perspective Articles Only:

_____ First 100 Reprints (free; black/white or color)

_____ Covers \$ _____

Subtotal \$ _____

Sales Tax* \$ _____

Total \$ _____

* For orders shipped to the following locations, please add the appropriate sales tax: Canada – 5%; in the US: CA – 8.25% plus the city and county rate; CT – 6%; DC – 6%; FL – 6% sales tax plus local surtax, if you are in a taxing county; MD – 6%; NC – 4.5%; NY – state and local sales taxes apply; VA – 5%; WI – 5%. A copy of the state sales tax exemption certificate must accompany the order form; otherwise sales tax will be assessed (billed).

3 Publication Fees (Research Articles Only)

Pages in article @ \$70 per page requested \$ _____

Color figures or tables in article @ \$300 each \$ _____

Replacement or deletion of color figures @ \$150 each \$ _____

Replacement of black/white or SI figures @ \$25 each \$ _____

Supporting information @ \$250 per article \$ _____

Open Access option @ \$1200 (\$850 if your institution has a 2009 Site License/Open Access Membership) per article \$ _____

Subtotal \$ _____

TOTAL AMOUNT due for reprint and publication fees \$ _____

4 Invoice Address It is PNAS policy to issue one invoice per order.

Name _____

Institution _____

Department _____

Address _____

City _____ State _____ Zip _____

Country _____

Phone _____ Fax _____

Purchase Order Number _____

5 Shipping Address (if different from Invoice Address)

Name _____

Institution _____

Department _____

Address _____

City _____ State _____ Zip _____

Country _____

Quantity of Reprints _____

Phone _____ Fax _____

6 Additional Shipping Address †

Name _____

Institution _____

Department _____

Address _____

City _____ State _____ Zip _____

Country _____

Quantity of Reprints _____

Phone _____ Fax _____

†Add \$45 for each additional shipping address.

7 Method of Payment

☐ Credit Card ☐ Personal Check (enclosed) ☐ Institutional Purchase Order (enclosed)

8 Credit Card Payment Details

Total Due _____

☐ Visa ☐ MasterCard ☐ AMEX

Card Number _____

Exp. Date _____

Signature _____

9 Payment Authorization

☐ I assume responsibility for payment of these charges.
(Signature is required. By signing this form, the author agrees to accept responsibility for payment of all charges described in this document.)

Signature of Responsible Author _____

Phone _____ Fax _____

3545220 09-11789

Reprint Order Number _____ Manuscript Number _____

Send payment and order form to **PNAS Reprints**, PO Box 631694, Baltimore, MD 21263-1694 FEIN 53-0196932
Please e-mail billmanj@cadmus.com, call 1-866-HURLOCK (toll free) or 1-410-943-3086 or fax 1-877-705-1373 if you have any questions.